Optimization of adsorption and sonocatalytic degradation of fluoride by zeolitic imidazole framework-8 (ZIF-8) using RSM-CCD

Nahid Khoshnamvand[a,b], Ali Jafari[a], Bahram Kamarehie[a], Maryam Faraji[c,d,*]

[a]*Department of Environment Health Engineering, Faculty of Health, Lorestan University of Medical Sciences, Lorestan, Iran,*
emails: nahidkhoshnam92@gmail.com (N. Khoshnamvand), jafari_a99@yahoo.com (A. Jafari), b.kamarehie@gmail.com (B. Kamarehie)
[b]*Department of Environmental Health Engineering, School of Public Health, Tehran University of Medical Sciences, Tehran, Iran*
[c]*Environmental Health Engineering Research Center, Kerman University of Medical Sciences, Kerman, Iran,*
email: M_faraji28@yahoo.com
[d]*Department of Environmental Health, School of Public Health, Kerman University of Medical Sciences, Kerman, Iran*

abstract

Fluorine is found in high concentrations in the earth's crust and in the groundwater. In this research, fluoride adsorption at the concentrations of 1–10 mg/L in the aqueous solutions was optimized by response surface methodology using sonocatalyst process in a frequency of 30 kHz by zeolitic imidazole framework-8 (ZIF-8) in dosage between 0.01 and 0.09 g/L, and pH from 3 to 11. According to the results, optimum conditions with removal efficiency of 92.17% was found at the fluoride concentration of 1.2 mg/L, ZIF-8 dosage of 0.08 g/L, and pH 6.52. Experimental data were well fitted on the Freundlich model ($R^2 = 0.99$); therefore, the adsorption was multilayer with a favorable affinity between fluoride and ZIF-8. The maximum adsorption capacity of ZIF-8 was obtained to be 33.11 mg/g. Also, the pseudo-second order model had the best agreement with data ($R^2 = 0.99$). Finally, this study demonstrated that the sonocatalyst process in combination with ZIF-8 is a promising and efficient method for adsorption of fluoride from aqueous solutions.

Keywords: Fluoride; Aqueous solutions; Zeolitic imidazole framework-8 (ZIF-8); Central composite design (CCD); Groundwater

1. Introduction

Fluoride is one of the elements in drinking water, which can impose effects on the human health depending on the concentration and exposure duration. In the last three decades, several studies have reported the dental and skeletal fluorosis due to the presence of fluoride ion more than the WHO guideline, that is, 1.0–1.5 mg/L [1]. Fluoride has been found above the concentration limit provided by WHO guideline in several cities in Iran, for example in Mashhahd, Yazd, Shiraz and Zahedan [2,3]. Also, fluoride concentration above the WHO guideline has been reported in the drinking water of several countries [4–8]. Therefore, the high concentration of fluoride in water bodies has been considered as a universal problem, mainly in the groundwater and the hence removal of fluoride from the water sources is a major challenge for public health.

The conventional methods have been applied for removal of fluoride from water resources included chemical precipitation, adsorption, ion exchange, reverse osmosis, electro coagulation and nano-filtration [9–11]. Advanced oxidation process (AOP) as an efficient method is broadly applied to remove the different pollutants in aqueous solutions [12]. The usage of ultrasonic waves for mechanical mixing has been considered as a new method in the AOPs. It can intensify the

* Corresponding author.

production of free radicals such as (•O, •OH, •H) or oxidizing agents such as hydrogen peroxide [13]. The existence of a catalyst can improve the breakdown of pollutants during the cavitation mechanism through further nuclei and increase the number of collisions [14]. Today, it is suggested to apply the low cost and novel adsorbents for treatment of pollutants in the water and wastewater [15]. Zeolitic imidazole frameworks (ZIFs) consist of mineral part of zinc metal (ZnN_4) and the organic part (2-methylimidazole), and are novel adsorbents among metal-organic frameworks (MOFs) [16]. MOFs have been successfully used for the removal of several pollutants including methylene blue dye [17], arsenic [18], fluoride [19–21] and antibiotic [22]. To the best of our knowledge, there has been no research regarding the fluoride adsorption under the sonocatalyst process by using ZIF-8 from aqueous solutions.

2. Materials and methods

2.1. ZIF-8 synthesis

0.59 g of $Zn(NO_3)_2 \cdot 6H_2O$ and 1.30 g of 2-methylimidazole (2-MIM) were added into 40 mL of deionized water to synthesize ZIF-8. Then, this solution was mixed for 4 h at 20°C. The products were separated by using centrifugation, washing with deionized water drying at 60°C for 24 h, and then, keeping it in a desiccator until use [23].

Characterizations of the ZIF-8 was analyzed by using scanning electron microscope coupled with the energy-dispersive X-ray spectroscopy (SEM-EDX) (HITACHI Model S-4160, Germany), X-ray diffraction (XRD) (Philips, Model XPERT PW 3040/60, The Netherlands) and Fourier transform infrared spectroscopy (FTIR) (HP 6890).

2.2. Experimental design

Response surface methodology (RSM) was used to study the effect of independent variables (Table 1) on the response (fluoride removal efficiency) and optimize the value of variables.

RSM is a complex of the mathematical and statistical approaches that are used to optimize processes. The main advantages of this approach are the reduced number of experiments, calculating the complex interaction between the independent variables, analysis and optimization as well as the improvement of existing design [24].

This method applies the central composite design (CCD) as an experimental design to fit a model by the technique of least squares. In this method, significant variables are determined in a factorial design. Then, experiments are designed

according to the Montgomery method in a rotatable CCD for independent variables [25]. An empirical second order polynomial regression model is set on the experimental method results (Eq. (1)):

$$Y = \beta_0 + \sum_{j=1}^{k} \beta_j x_j + \sum_{j=1}^{k} \beta_{jj} x_j^2 + \sum \sum_{i<j=2}^{k} \beta_{ij} x_i x_j \qquad (1)$$

where Y shows the response; x_i and x_j are independent variables (i and j ranging from 1 to k); β_0 is the constant term; β_j is the linear coefficient, β_{ij} is the interaction coefficient, and β_{jj} is the quadratic coefficient; k is the number of independent variables ($k = 3$ in the current study) [24].

2.3. Batch adsorption studies

Batch adsorption studies were investigated based on the experimental design in triplicate. pH values were adjusted by using H_2SO_4 or NaOH (1 N). Also, NaF (2.21 g) was dissolved in the distilled water (1,000 mL) to prepare a stock solution of fluoride.

Fluoride solutions at different concentrations, ZIF-8 dosages, and pH values were agitated by magnetic stirrer at 200 rpm, and then sonicated in an ultrasonic bath (Elma Ultrasonic model TI-H-25, Germany) at 30 kHz for 45 min. After that elapsed, the samples were filtered (0.45 μm, Whatman filter paper) and the residual fluoride concentration was analyzed by a UV-visible spectrophotometer (PerkinElmer, Lambda 25, United States) at a maximum wavelength of 570 nm according to the standard methods for the examination of water and wastewater [26]. The amount of the adsorbed fluoride at equilibrium (q_e) and as well as the fluoride removal efficiency (Y) was calculated using Eqs. (2) and (3), respectively:

$$q_t = \frac{V}{M}\left(C_0 - C_e\right) \qquad (2)$$

$$Y\left(\%\right) = \frac{C_0 - C_e}{C_0} \times 100 \qquad (3)$$

where C_e and C_0 are the equilibrium and initial concentrations of fluoride (mg/L), respectively, q_e is the adsorbed fluoride on the adsorbent (mg/g) at the equilibrium conditions, V is the volume of the solution (L), M is the mass of the adsorbent (g), and Y is the removal efficiency [27].

Table 1
Independent variables and their levels (coded and uncoded)

Independent variables	Unit	Symbol	Level of variables				
			−1.68	−1	0	+1	+1.68
Fluoride concentration	mg/L	X_1	1	2.82	5.5	8.18	10
ZIF-8 dosage	g/L	X_2	0.01	0.03	0.05	0.07	0.09
pH	–	X_3	3	4.62	7	9.38	11

2.4. Statistical analysis

The relationship between the independent variables and response was explored in the multiple regression analysis through the generalized least square using the Design-Expert software (version 10). The mean difference of fluoride removal between independent variables was compared in a two-way analysis of variance (ANOVA) test. The p-value less than 0.05 was defined as a significant level.

3. Results

3.1. ZIF-8 characterization

The SEM and EDX images are shown in Figs. 1a and b, respectively. Fig. 2 presents the XRD pattern of ZIF-8. FTIR spectrum of ZIF-8 is displayed in Fig. 3.

3.2. Central composite statistical analysis

The results of CCD and fluoride removal percentage in terms of predicted and actual responses are represented in Table 2. Second order model was considered as the best regression model between input variables and fluoride removal percentage as the response.

Response was evaluated as a function of fluoride concentration (X_1), ZIF-8 dosage (X_2), and pH (X_3) and calculated as the sum of a constant, three first-order effects (X_1, X_2 and X_3), three interaction effects (X_1X_2, X_1X_3 and X_2X_3) and three second order effects (X_1^2, X_2^2 and X_3^2) (Eq. (1)). ANOVA results for the fitted polynomial model are presented in Table 3. The fitness between predicted and actual responses is shown in diagnostics plot in Fig. 4. The p-value for lack of fit was gained to be insignificant (p-values > 0.05).

Coefficients of the second order model were estimated through the procedure of multiple regression analysis in RSM. The fitted model in terms of the actual factors for the
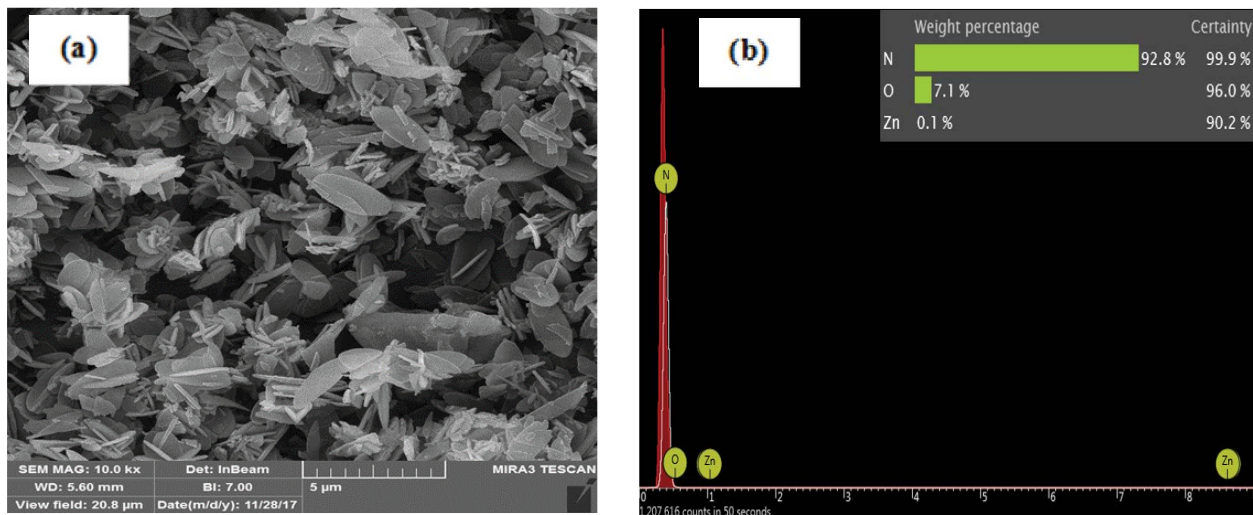
Fig. 1. Characterization of ZIF-8, (a) SEM image, (b) EDX image.
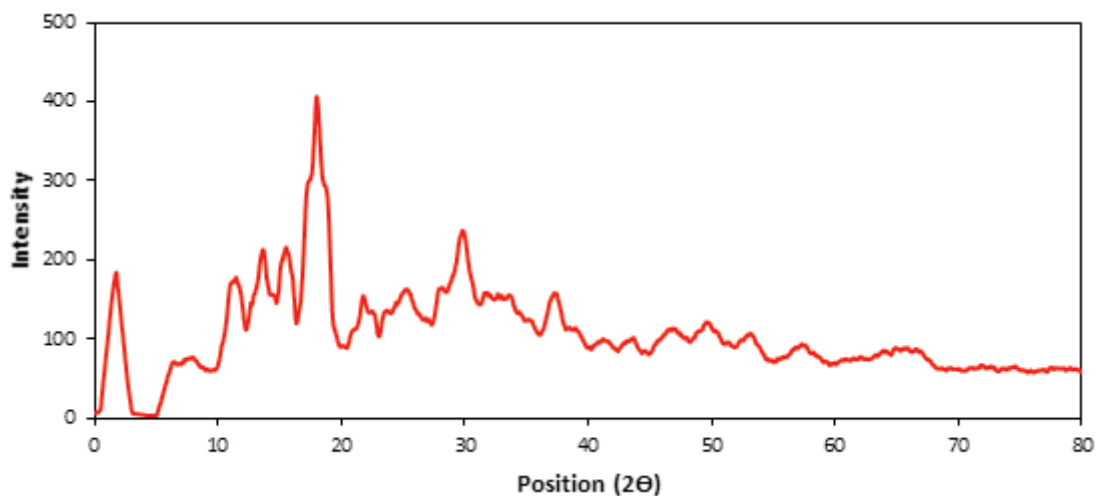
Fig. 2. XRD pattern of ZIF-8.
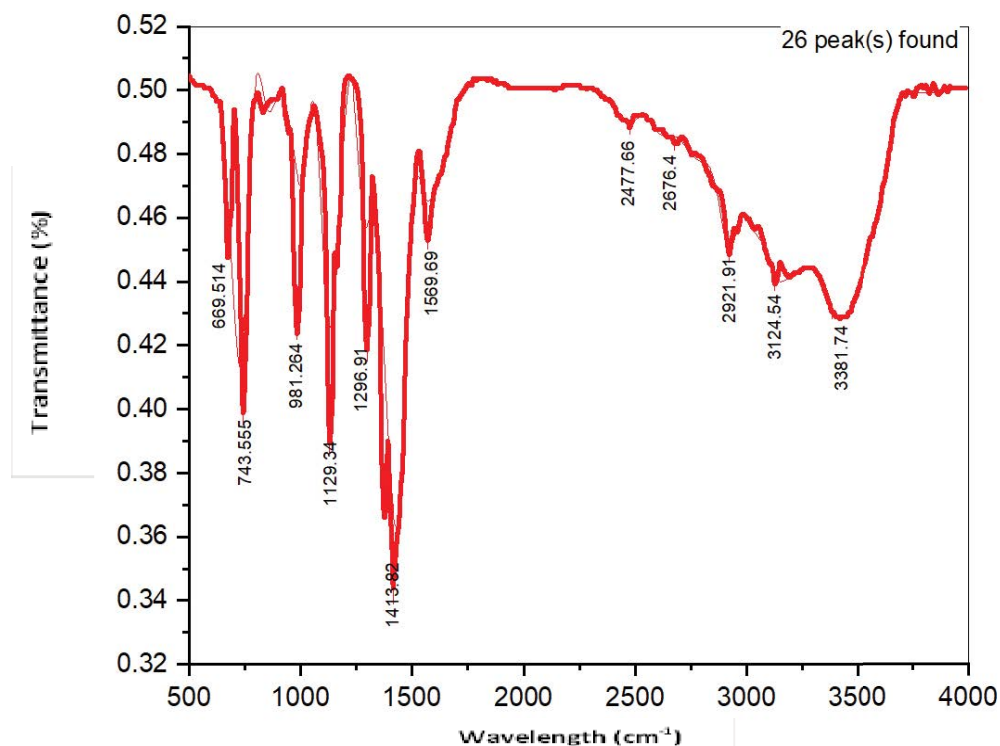
Fig. 3. FTIR spectrum of ZIF-8. *X* axis: wavelength (cm⁻¹). *Y* axis: transmittance (%).

Table 2
Central composite design (CCD) and observed responses for fluoride removal

Run	Coded variables			Actual variables			Fluoride removal (%)	
	X_1	X_{2+}	X_3	Fluoride concentration	ZIF-8 dosage	pH	Experimental	Predicted+
1	0	0	−1.68	5.50	0.05	3.00	83	87
2	0	0	0	5.50	0.05	7.00	82	84
3	−1	1	1	2.82	0.07	9.38	86	91
4	0	0	0	5.50	0.05	7.00	77	84
5	1	−1	1	8.18	0.03	9.38	57	58
6	0	−1.68	0	5.50	0.01	7.00	75	75
7	−1	−1	1	2.82	0.03	9.38	75	75
8	−1	1	−1	2.82	0.07	4.62	85	89
9	1	−1	−1	8.18	0.03	4.62	87	87
10	0	1.68	0	5.50	0.09	7.00	82	94
11	1	1	−1	8.18	0.07	4.62	85	94
12	0	0	0	5.50	0.05	7.00	81	84
13	−1	−1	−1	2.82	0.03	4.62	81	82
14	−1.68	0	0	1.00	0.05	7.00	85	89
15	0	0	0	5.50	0.05	7.00	77	84
16	0	0	0	5.50	0.05	7.00	84	84
17	0	0	1.68	5.50	0.05	11.00	58	64
18	0	0	0	5.50	0.05	7.00	80	84
19	1.68	0	0	10.00	0.05	7.00	76	79
20	1	1	1	8.18	0.07	9.38	66	74

Table 3
Analysis of variance (ANOVA) results for the fitted polynomial model for fluoride removal in sonocatalyst process by ZIF-8

Source	Sum of squares	df	Mean square	p-value
Model	1,355.45	9	150.61	<0.0001
X_1	162.69	1	162.69	0.0004
X_2	78.6	1	78.60	0.0044
X_3	675.46	1	675.46	<0.0001
X_1X_2	8	1	8	0.27
X_1X_3	242	1	242	<0.0001
X_2X_3	40.5	1	40.50	0.0253
X_1^2	2.46	1	2.46	0.5317
X_2^2	1.56	1	1.56	0.6172
X_3^2	140.49	1	140.49	0.0006
Residual	58.67	10	5.87	
Lack of fit	19.03	5	3.81	0.78
Pure error	39.63	5	7.93	

Note: X_1: Fluoride concentration, X_2: ZIF-8 dosage, X_3: pH. R^2: 0.95, Adjusted R^2: 0.92, Predicted R^2: 0.90.
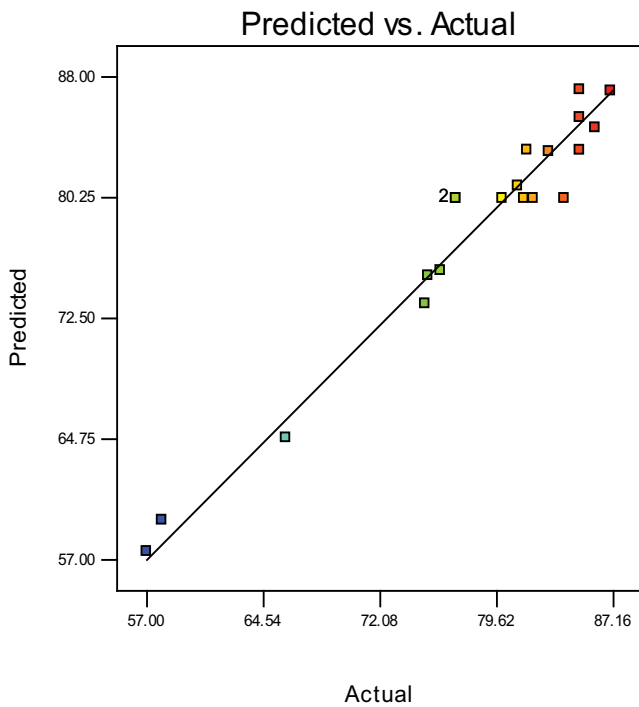
Fig. 4. Diagnostic plot of removal efficiency; predicted vs. actual.

significant coefficients is shown in Table 3 (p-values < 0.05) is given by Eq. (4):

$$Y\left(\text{fluoride Removal}(\%)\right) = +52.51 + \left(4.91 \times X_1\right) - \left(32.94 \times X_2\right) + \left(7.53 \times X_3\right) - \left(0.86 \times X_1 \times X_3\right) + \left(39.77 \times X_2 \times X_3\right) - \left(0.55 \times X_3^2\right) \quad (4)$$

where X_1, X_2 and X_3 are fluoride concentration, ZIF-8 dosage, and pH, respectively.

3.3. Validation of the model

According to the numerical optimization results, predicted maximum efficiency based on the fitted regression model (Eq. (4)) was found to be 90.67% in the optimum value of variables, that is, 1.2 mg/L, 0.08 g/L and 6.52 for fluoride concentration, ZIF-8 dosage, and pH, respectively. The experimental fluoride removal efficiency based on the optimum conditions obtained was attained to be 92.17% in triplicate experiments.

3.4. Effect of various parameters on the fluoride removal efficiency

Contour plots of significant two-way interactions according to Table 3, that is, fluoride concentration with pH and ZIF-8 with pH are graphically displayed in Figs. 5a and b, respectively. In these plots, the effect of two variables on the
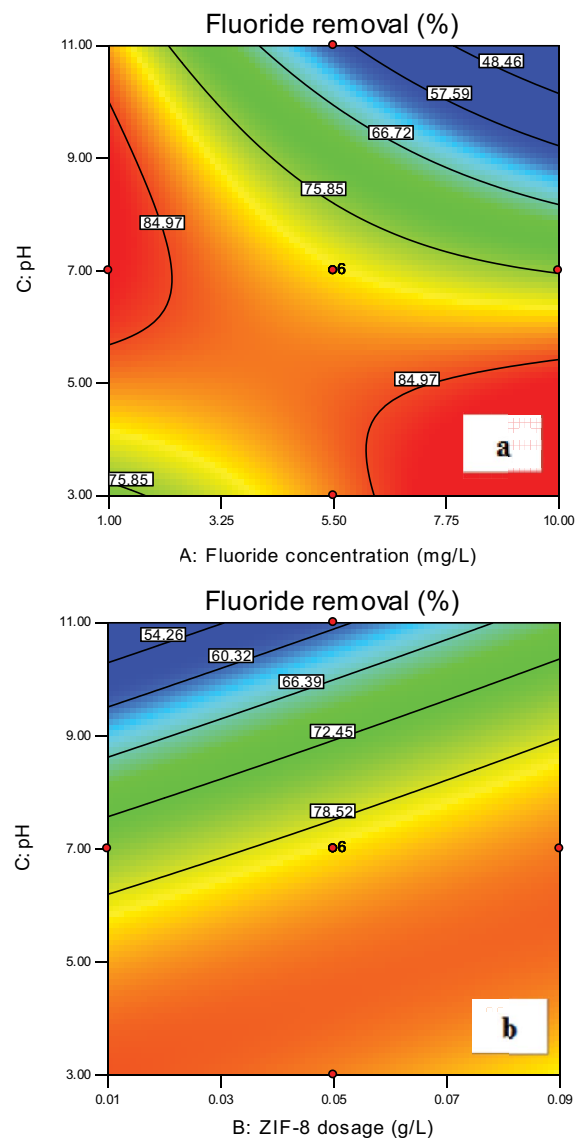
Fig. 5. Contour plots of fluoride removal (%) as a function of (a) fluoride concentration and pH, (b) ZIF-8 dosage and pH.

removal efficiency is plotted, while the third variable is at the fixed central level.

3.5. Effect of fluoride concentration on the fluoride removal

Contour plot of fluoride removal (%) as a function of fluoride concentration from 1 to 10 mg/L and pH between 3 and 11 is visualized in Fig. 5a. An increased initial fluoride concentration was resulted into the decrease removal efficiency.

3.6. Effect of ZIF-8 dosage on the fluoride removal

Removal efficiency is compared in the different ZIF-8 dosages in the range of 0.01–0.09 g/L and pH from 3 to 11 in Fig. 5b. Fluoride removal was improved in the ZIF-8 dosage between 0.01 and 0.08 g/L. Then, efficiency was reduced in the ZIF-8 dosage more than mentioned range.

3.7. Effect of pH on the fluoride removal

Also, Figs. 5a and b have depicted the effect of pH between 3 and 11 on the fluoride removal at the different fluoride concentrations and ZIF-8 dosages, respectively. In both plots, increased efficiency was obtained in the pH range from 3 to 6.52 and it was decreased in pH values higher than 6.52.

3.8. Isotherm study

In the present study, four isotherm models including the Langmuir, Freundlich, Dubinin–Radushkevich and Temkin were analyzed. Information on the fitted isotherm models on experimental data is characterized in Table 4 and Figs. 6a–d. As seen in Table 4, the value of R^2 for the Freundlich model is maximum compared with other isotherm models ($R^2 = 0.99$). The n value was found to be 2.22 (Table 4). The maximum adsorption capacity (q_{max}) of ZIF-8

for the fluoride adsorption in the current study was found to be 33.11 mg/g according to the Eq. (5):

$$K_f = \frac{q_m}{C_0^{\frac{1}{n}}} \tag{5}$$

where K_f is Freundlich adsorption constant (L/mg), q_m is the Freundlich maximum adsorption capacity (mg/g), C_0 is the initial concentration of the solute in the bulk solution (mg/L) and n is sorption capacity [28]. Maximum capacity of different adsorbents for fluoride adsorption is compared in Table 5.

3.9. Kinetic modelingW

Results of the fluoride removal efficiency at the concentrations of 1–10 mg/L during 10–45 min in the adsorbent dosage and pH value in optimum points were fitted on the four kinetic models, that is, pseudo-first order, pseudo-second order, intraparticle diffusion and Elovich. Other variables included ZIF-8 dosage and pH were set in the obtained optimum contents. Table 6 and Figs. 7a–d explain findings from the kinetic study. According to Table 6, the pseudo-second order kinetic model had bigger R^2 values ($R^2 = 0.99$), then it could be concluded that this model had a better agreement on the experimental data.

4. Discussion

Leaf-shaped ZIF-8 is shown in Fig. 1a. Condition of synthesis and type of solvent can affect the morphology of ZIF-8. Synthesized ZIF-8 in the present study had a mean particle size of 5,000 nm according to the SEM analysis. Main elements in the ZIF-8 were detected in EDX analysis (Fig. 1b) as nitrogen (N), oxygen (O) and zinc (Zn) with a weight percentage of 92.8%, 7.1% and 0.1%,

Table 4
Results of isotherm study

Model	Formula	Linear form	Plot	Parameter	Value
Langmuir	$q_e = q_m \cdot b \cdot C_e / 1 + k_L \cdot C_e$	$C_e/q_e = C_e/q_m + 1/q_m \cdot k_L$	C_e/q_e vs. C_e	q_{max} (mg/g)	22.73
				k_L (L/mg)	0.29
				R^2	0.87
Freundlich	$q_e = k_f C_e^{1/n}$	$\log q_e = \log k_f + 1/n \log C_e$	$\log q_e$ vs. $\log C_e$	K_f (L/mg)	5.01
				n	2.22
				q_{max} (mg/g)	33.11
				R^2	0.99
Temkin	$q_e = RT/b \ln (k_t \cdot C_e)$	$q_e = B_1 \ln k_t + B_1 \ln C_e$	q_e vs. $\ln C_e$	K_t (L/mg)	7.14
				B_1	3
				R^2	0.94
Dubinin–Radushkevich	$q_e = q_m \exp. (-B.\varepsilon^2)$	$\ln q_e = \ln q_m - B \cdot \varepsilon^2$	$\ln q_e$ vs. ε^2	q_{max} (mg/g)	7.39
				B	0.0002
				E (kJ/mol)	50
				R^2	0.89
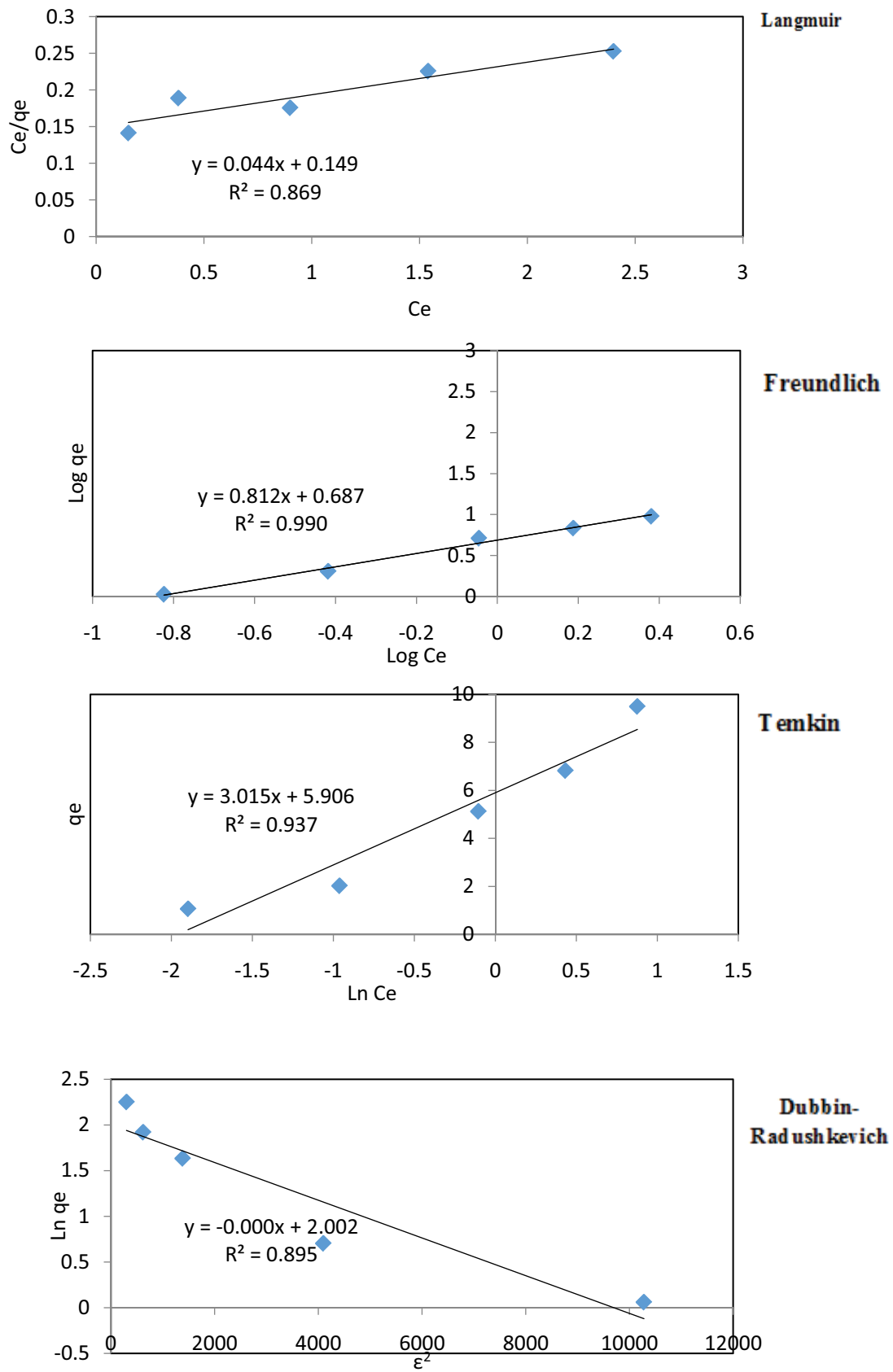
Fig. 6. Fitting the experimental data with isotherm models.

Table 5
Comparative investigation of maximum adsorption capacity of fluoride using different adsorbents

Adsorbent	Maximum adsorption capacity (mg/g)	Reference
Uio-66 functionalized with amine groups	41.5	[19]
ZIF-8	25	[21]
Uio-66	20	[21]
Metal organic frameworks	31	[20]
ZIF-8	33.11	This study

Table 6
Results of kinetic study

Model	Formula	Plot	Parameter	Fluoride concentration (mg/L)				
				1	3	5	8	10
Pseudo-first order	$\log(q_e - q_t) = \log q_e - k_1 \cdot t$	$\log(q_e - q_t)$ vs. t	K_1 (min^{-1})	0.03	0.04	0.02	0.01	0.03
			q_e (cal) (mg/g)	0.57	0.97	1.14	1.31	1.86
			R^2	0.97	0.88	0.87	0.99	0.99
Pseudo-second order	$t/q_t = 1/k_2 \cdot q_e^2 + (t/q_e)$	t/q_t vs. t	K_2 (min^{-1})	0.34	0.08	0.04	0.03	0.02
			q_e (cal) (mg/g)	0.9	3.3	4.5	7.1	9.1
			R^2	0.99	0.99	0.99	0.99	0.99
Intraparticle diffusion	$q_t = k_p \cdot t^{0.5} + c$	q_t vs. $t^{0.5}$	K_p (mg/g min$^{-0.5}$)	0.04	0.1	0.24	0.36	0.61
			C (mg/g)	0.58	1.8	2.37	3.75	3.6
			R^2	0.99	0.95	0.93	0.96	0.98
Elovich	$q_t = 1/\beta \ln(\alpha \cdot \beta) + 1/\beta \ln t$	q_t vs. $\ln t$	β (g/mg)	11.11	4.35	1.79	1.23	0.7
			α (mg/g min^{-1})	18.67	194.95	15.26	32.13	6.09
			R^2	0.98	0.94	0.86	0.91	0.99

respectively. The major peaks in the XRD pattern (Fig. 2) were detected at 2θ among 1°, 18° and 30°. Strong peaks in the mentioned range could be a proper indicator to show the crystallization of the adsorbent. The XRD pattern of the ZIF-8 synthesized in the current study was consistent to another study [29].

FTIR spectra in Fig. 3 in the range of 600–4,000 cm^{-1} were attributed to the ligand 2-MIM. These peaks were in accordance with other studied [30]. Peaks from 600 to 1,500 cm^{-1} can be allocated to stretching and bending types of the imidazole ring. The peak at 1,569 cm^{-1} was related to the stretching bond of C=N in 2-MIM. Peaks at 1,178 cm^{-1} can be assigned the C–N stretching bond [30]. Peaks at 2,925 and 3,137 cm^{-1} may be achieved from the stretching mode of C–H in 2-MIM, inside the aromatic ring and the aliphatic chain, respectively. Peaks from 3,000 to 3,500 cm^{-1} were associated to the water. A broad peak at ~3,400 cm^{-1} approved the symmetric and asymmetric stretching bonds of H$_2$O [31,30].

Second order polynomial model was fitted between the actual responses obtained from the experiments and independent variables presented in Table 2. Based on the adjusted correlation coefficients value (R^2) equal to 0.92, it could be concluded that there was an acceptable correlation between predicted responses from the fitted model and actual data from experimental studies. Also, a good fitness between predicted and actual responses is visualized in

Fig. 4. A high value of R^2 cannot approve that the best model is selected. Therefore, the lack of fit can be a useful index to select the accurate regression model. Lack of fit value would be calculated through the difference between of sum of the squares for the actual response and its predicted values from the fitted model. An insignificant lack of fit was favorite (p-value > 0.05) because it showed the validation of model [24]. According to Table 3, the insignificant lack of fit with a p-value equal to 0.78 showed that the model could accurately predict responses. As seen in Table 3, all independent variables included fluoride concentration, ZIF-8 dosage, and pH had a significant effect (p-value < 0.05) on the fluoride removal in the present study.

Based on Fig. 5a, fluoride removal was attenuated by the increased fluoride concentration. This finding could be justified due to the more active sites on the adsorbent surface at the lower fluoride concentrations. Our result was in accordance to the other studies [32–34].

The increased dosage of ZIF-8 seriously improved the fluoride adsorption (Fig. 5b). The increased adsorption with an increased ZIF-8 dosage could be assigned to the higher surface area and more accessible active sites and also additional nuclei for the production of cavitation bubbles [35]. But, adsorption was decreased in the ZIF-8 dosage more than optimum value of 0.08 g/L, possibly due to the aggregation of ZIF-8 particles and consequently restriction of the active sites that contribute to the production of •OH in the solution.
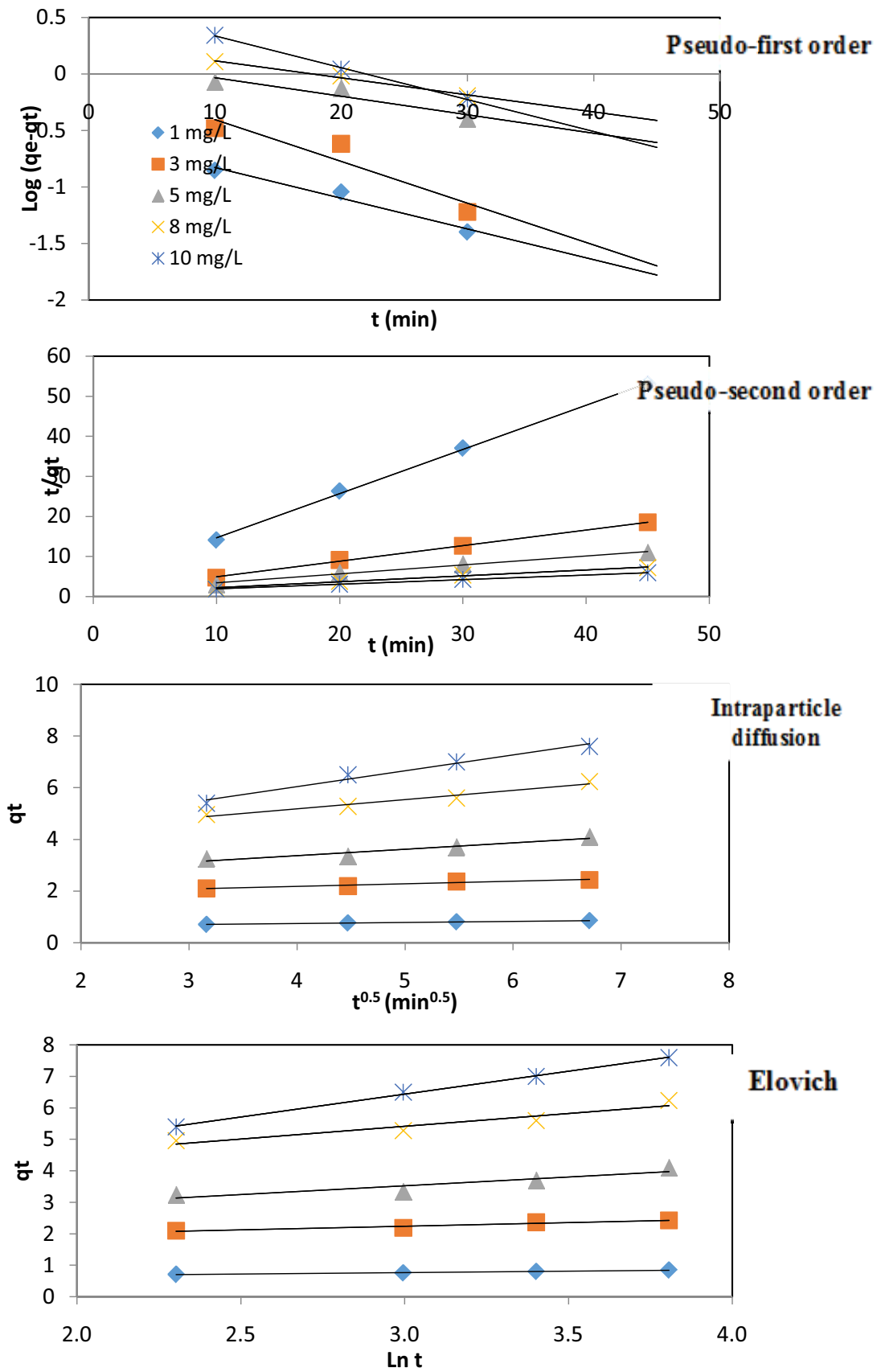
Fig. 7. Fitting the experimental data with kinetic models.

Moreover, ultrasonic irradiation may scatter close to the catalyst surface in the further contents of catalyst, so the degradation rate of sonocatalytic could be limited. In addition, increased sonocatalyst can consume •OH at the interface of liquid–gas. Furthermore, higher dosages of sonocatalyst would produce the weak collapse of bubbles and reduce the production of •OH due to the accumulation of sonocatalytic by-products in the cavitation bubbles [35].

Based on Figs. 5a and b, increasing pH from 3 to 6.52 (optimum point) augmented fluoride removal efficiency. According to the pH of zero-point charge (pHzpc) for ZIF-8 equal to 9.6 [13,16], the fluoride adsorption mechanism in pH values between 3 and 6.52 could be attributed to changing of the surface charge in the ZIF-8 and electrostatic attraction. Other studies have also concluded that removal efficiency may be decreased by increasing the solution pH [36,37]. A smaller efficiency in the acidic pH could be associated to dissolve the ZIF-8 in this pH range [16].

In the isotherm studies, the Freundlich was selected as the best isotherm model due to a higher value of R^2 compared with other models (Table 4). Therefore, the fluoride adsorption was multilayer and fluoride molecules responded first with the surface of ZIF-8 and after that with each other. The n index in the Freundlich model characterizes adsorption intensity that its value in the range of 2–10 indicates a favorable adsorption process [38]. So, the n value equal to 2.22 in this study (Table 4) represented a favorable adsorption process. The affinity between fluoride and ZIF-8 can be determined through R_L (dimensionless) in the Langmuir model from Eq. (6):

$$R_L = \frac{1}{1 + bC_0} \qquad (6)$$

where C_0 and b are the fluoride concentration (mg/L) and the Langmuir isotherm constant (L/mg), respectively.

Adsorption process can be categorized according to the R_L value as follows: unfavorable ($R_L > 1$), linear ($R_L = 1$), favorable ($0 < R_L < 1$), or irreversible ($R_L = 0$) [39]. The average of this parameter was found to be 0.53 in this study that approved the process of fluoride adsorption was favorable through applied adsorbent under the conditions of this research.

The pseudo-second order model had a larger R^2 value (Table 6), then it could be stated that this model had a better agreement with the experimental data in this studies. Dominant of the pseudo-second order model showed that chemisorption process was the key mechanism in the adsorption process in current study [37]. Similarly in the study of Shams et al. [13] on the adsorption of phosphorus by cubic zeolitic imidazolate framework-8, the pseudo-second order model had a better fitness on the experimental data.

5. Conclusions

Results of the current study showed that sonocatalyst process by the ZIF-8 had a good efficiency for fluoride removal from aqueous solutions. Process had a maximum efficiency of fluoride removal (92.17%) in the pH value = 6.52, ZIF-8 dosage = 0.08 g/L and fluoride concentration = 1.2 mg/L.

A good fitness of the Freundlich model on the experimental data approved a multilayer adsorption process with the maximum capacity of 33.11 mg/g. According to fitness of the pseudo-second order model on data, the chemisorption process was considered as the fundamental mechanism in the adsorption process. Findings showed that the sonocatalyst process in combination with ZIF-8 as the catalyst in examined conditions could efficiently remove fluoride from aqueous solutions.

Acknowledgments

References

[1] World Health Organization, Guidelines for Drinking-Water Quality, World Health Organization, 2004.

[2] A. Mesdaghinia, K.A. Vaghefi, A. Montazeri, M.R. Mohebbi, R. Saeedi, Monitoring of fluoride in groundwater resources of Iran, Bull. Environ. Contam. Toxicol., 84 (2010) 432–437.

[3] M.H. Dehghani, G.A. Haghighat, M. Yousefi, Data on fluoride concentration in drinking water resources in Iran: a case study of Fars province; Larestan region, Data Brief, 19 (2018) 842–846.

[4] A.C. Samal, P. Bhattacharya, A. Mallick, M.M. Ali, J. Pyne, S.C. Santra, A study to investigate fluoride contamination and fluoride exposure dose assessment in lateritic zones of West Bengal, India, Environ. Sci. Pollut. Res., 22 (2015) 6220–6229.

[5] P. Näsman, F. Granath, J. Ekstrand, A. Ekbom, G. Sandborgh-Englund, C.M. Fored, Natural fluoride in drinking water and myocardial infarction: a cohort study in Sweden, Sci. Total Environ., 562 (2016) 305–311.

[6] M. Arif, I. Hussain, J. Hussain, S. Sharma, S. Kumar, Fluoride in the drinking water of Nagaur Tehsil of Nagaur district, Rajasthan, India, Bull. Environ. Contam. Toxicol., 88 (2012) 870–875.

[7] K. Brindha, L. Elango, Fluoride in groundwater: causes, implications and mitigation measures, Fluoride Pro. App. Environ. Manage., 1 (2011) 111–136.

[8] J. Bundschuh, J.P. Maity, S. Mushtaq, M. Vithanage, S. Seneweera, J. Schneider, P. Bhattacharya, N.I. Khan, I. Hamawand, L.R. Guilherme, Medical geology in the framework of the sustainable development goals, Sci. Total Environ., 581 (2017) 87–104.

[9] M.A. Zazouli, A.H. Mahvi, S. Dobaradaran, M. Barafrashtehpour, Y. Mahdavi, D. Balarak, Adsorption of fluoride from aqueous solution by modified *Azolla filiculoides*, Fluoride, 47 (2014) 349–358.

[10] S. Dobaradaran, I. Nabipour, A.H. Mahvi, M. Keshtkar, F. Elmi, F. Amanollahzade, M. Khorsand, Fluoride removal from aqueous solutions using shrimp shell waste as a cheap biosorbent, Fluoride, 47 (2014) 253–257.

[11] E. Bazrafshan, N. Khoshnamvand, A.H. Mahvi, Fluoride removal from aqueous environments by $ZNCl_2$-treated eucalyptus leaves as a natural adsorbent, Fluoride, 48 (2015) 315–320.

[12] M. Malakootian, M. Pourshaban-Mazandarani, H. Hossaini, M.H. Ehrampoush, Preparation and characterization of TiO_2 incorporated 13X molecular sieves for photocatalytic removal of acetaminophen from aqueous solutions, Process Saf. Environ. Protect., 104 (2016) 334–345.

[13] M. Shams, M.H. Dehghani, R. Nabizadeh, A. Mesdaghinia, M. Alimohammadi, A.A. Najafpoor, Adsorption of phosphorus from aqueous solution by cubic zeolitic imidazolate framework-8: modeling, mechanical agitation versus sonication, J. Mol. Liq., 224 (2016) 151–157.

[14] Y.L. Pang, A.Z. Abdullah, Fe^{3+} doped TiO_2 nanotubes for combined adsorption–sonocatalytic degradation of real textile wastewater, Appl. Catal., B, 129 (2013) 473–481.

[15] M. Malakootian, N.-a. Jaafarzadeh, H. Hossaini, Efficiency of perlite as a low cost adsorbent applied to removal of Pb and Cd from paint industry effluent, Desal. Wat. Treat., 26 (2011) 243–249.

[16] M. Jian, B. Liu, G. Zhang, R. Liu, X. Zhang, Adsorptive removal of arsenic from aqueous solution by zeolitic imidazolate framework-8 (ZIF-8) nanoparticles, Colloids Surf., A., 465 (2015) 67–76.

[17] A. Mohammadi, A. Alinejad, B. Kamarehie, S. Javan, A. Ghaderpoury, M. Ahmadpour, M. Ghaderpoori, Metal-organic framework Uio-66 for adsorption of methylene blue dye from aqueous solutions, Int. J. Environ. Sci. Technol., 14 (2017) 1959–1968.

[18] M. Massoudinejad, M. Ghaderpoori, A. Shahsavani, A. Jafari, B. Kamarehie, A. Ghaderpoury, M.M. Amini, Ethylenediamine-functionalized cubic ZIF-8 for arsenic adsorption from aqueous solution: modeling, isotherms, kinetics and thermodynamics, J. Mol. Liq., 255 (2018) 263–268.

[19] M. Massoudinejad, M. Ghaderpoori, A. Shahsavani, M.M. Amini, Adsorption of fluoride over a metal organic framework Uio-66 functionalized with amine groups and optimization with response surface methodology, J. Mol. Liq., 221 (2016) 279–286.

[20] M. Massoudinejad, A. Shahsavani, B. Kamarehie, A. Jafari, M. Ghaderpoori, M.M. Amini, A. Ghaderpoury, Highly efficient adsorption of fluoride from aqueous solutions by metal organic frameworks: modeling, isotherms, and kinetics, Fluoride, 51 (2018) 355–365.

[21] B. Kamarehie, Z. Noraee, A. Jafari, M. Ghaderpoori, M.A. Karami, A. Ghaderpoury, Data on the fluoride adsorption from aqueous solutions by metal-organic frameworks (ZIF-8 and Uio-66), Data Brief, 20 (2018) 799–804.

[22] A. Nasiri, F. Tamaddon, M.H. Mosslemin, M. Faraji, A microwave assisted method to synthesize nanoCoFe$_2$O$_4$@methyl cellulose as a novel metal-organic framework for antibiotic degradation, MethodsX, 6 (2019) 1557–1563.

[23] R. Chen, J. Yao, Q. Gu, S. Smeets, C. Baerlocher, H. Gu, D. Zhu, W. Morris, O.M. Yaghi, H. Wang, A two-dimensional zeolitic imidazolate framework with a cushion-shaped cavity for CO$_2$ adsorption, Chem. Commun., 49 (2013) 9500–9502.

[24] M. Malakootian, A. Nasiri, H. Mahdizadeh, Metronidazole adsorption on CoFe$_2$O$_4$/activated carbon@chitosan as a new magnetic biocomposite: modelling, analysis, and optimization by response surface methodology, Desal. Wat. Treat., 164 (2019) 215–227.

[25] A. Yazdanbakhsh, Y. Hashempour, M. Ghaderpouri, Performance of granular activated carbon/nanoscale zero-valent iron for removal of humic substances from aqueous solution based on experimental design and response surface modeling, Global Nest J., 20 (2018) 57–68.

[26] W.E. Federation, A.P.H. Association, Standard Methods for the Examination of Water and Wastewater, American Public Health Association (APHA), Washington, DC, USA, 2005.

[27] M. Malakootian, K. Yaghmaeian, M. Malakootian, Wood ash effectiveness in cadmium removal from paint industrial effluent, Pak. J. Biol. Sci., 9 (2006) 248–252.

[28] O. Hamdaoui, E. Naffrechoux, Modeling of adsorption isotherms of phenol and chlorophenols onto granular activated carbon: Part I. Two-parameter models and equations allowing determination of thermodynamic parameters, J. Hazard. Mater., 147 (2007) 381–394.

[29] N.A.H.M. Nordin, S.M. Racha, T. Matsuura, N. Misdan, N.A.A. Sani, A.F. Ismail, A. Mustafa, Facile modification of ZIF-8 mixed matrix membrane for CO$_2$/CH$_4$ separation: synthesis and preparation, RSC Adv., 5 (2015) 43110–43120.

[30] K.-Y.A. Lin, H.-A. Chang, Ultra-high adsorption capacity of zeolitic imidazole framework-67 (ZIF-67) for removal of malachite green from water, Chemosphere, 139 (2015) 624–631.

[31] M. Ghaedi, F.N. Azad, K. Dashtian, S. Hajati, A. Goudarzi, M. Soylak, Central composite design and genetic algorithm applied for the optimization of ultrasonic-assisted removal of malachite green by ZnO Nanorod-loaded activated carbon, Spectrochim. Acta, Part A, 167 (2016) 157–164.

[32] G. El-Sayed, H. Dessouki, H. Jahin, S. Ibrahiem, Photocatalytic degradation of metronidazole in aqueous solutions by copper oxide nanoparticles, J. Basic Environ. Sci., 1 (2014) 102–110.

[33] H.-G. Guo, N.-Y. Gao, W.-H. Chu, L. Li, Y.-J. Zhang, J.-S. Gu, Y.-L. Gu, Photochemical degradation of ciprofloxacin in UV and UV/H$_2$O$_2$ process: kinetics, parameters, and products, Environ. Sci. Pollut. Res., 20 (2013) 3202–3213.

[34] F. Mostafapour, E. Bazrafshan, D. Belark, N. Khoushnamvand, Survey of Photo-catalytic degradation of ciprofloxacin antibiotic using copper oxide nanoparticles (UV/CuO) in aqueous environment, J. Rafsanjan Univ. Med. Sci. Health Ser., 15 (2016) 307–318.

[35] R.D.C. Soltani, S. Jorfi, H. Ramezani, S. Purfadakari, Ultrasonically induced ZnO–biosilica nanocomposite for degradation of a textile dye in aqueous phase, Ultrason. Sonochem., 28 (2016) 69–78.

[36] M. Mourabet, A. El Rhilassi, H. El Boujaady, M. Bennani-Ziatni, R. El Hamri, A. Taitai, Removal of fluoride from aqueous solution by adsorption on hydroxyapatite (HAp) using response surface methodology, J. Saudi Chem. Soc., 19 (2015) 603–615.

[37] H. Nourmoradi, A. Ebrahimi, Y. Hajizadeh, S. Nemati, A. Mohammadi, Application of nanozeolite and nanocarbon for the removal of humic acid from aqueous solutions, Int. J. Pharm. Technol., 8 (2016) 13337–13352.

[38] N. Khoshnamvand, E. Bazrafshan, B. Kamarei, Fluoride removal from aqueous solutions by NaOH-modified eucalyptus leaves, J. Environ. Health Sustain. Dev., 3 (2018) 481–487.

[39] M. Malakootian, A. Nasiri, H. Mahdizadeh, Preparation of CoFe$_2$O$_4$/activated carbon@ chitosan as a new magnetic nanobiocomposite for adsorption of ciprofloxacin in aqueous solutions, Water Sci. Technol., 78 (2018) 2158–2170.